

Numerical Simulation and Characteriation of Pentacene based Organic Thin Film Transistors with Top and Bottom Gate Configurations

Pooja Kumari¹ and A. D. D. Dwivedi²

¹ Poornima University Jaipur

Received: 13 December 2018 Accepted: 5 January 2019 Published: 15 January 2019

Abstract

In this paper, we model the characteristics of top and bottom gate configurations of organic thin film transistors (OTFTs) including top gate top contact (TGTC), top gate bottom contact (TGBC), bottom gate top contact (BGTC), bottom gate bottom contact (BGBC). The path of charge carriers changes in different geometries which possess difference in the electrical behaviour of the devices. The performances of bottom and top gate pentacene based OTFT devices have been analyzed and their performance parameters like mobility, threshold voltage, sub threshold slope, trans conductance, on off ratio have been extracted and compared. **Keywords:** organic thin film transistors (OTFTS), numerical simulation, pentacene, top gate top contact (TGTC), top gate bottom contact (TGBC), bottom gate top contact (BGTC) and bottom gate bottom contact (BGBC).

Index terms— organic thin film transistors (OTFTS), numerical simulation, pentacene, top gate top contact (tgtc),

Introduction rganic electronics is the field which is fast developing in today's scenario. Organic semi-conductors (OSC) have made the device low cost and made the field of organic electronics active. Organic transistors can be directly fabricated on flexible cheap substrates and it requires low temperature which makes the device cost efficient. Various researchers used the flexible substrates like glass [1] and plastic [2] which led the fabrication cost very low. Organic thin film transistors have been used in various applications like Organic light emitting diodes (OLEDs) [3], Organic displays [4], Organic radio frequency identification tags [5][6][7][8][9][10][11][12][13][14][15][16][17][18][19][20][21][22][23], organic sensors [6][7][8][9][10][11][12][13][14][15][16][17][18][19][20][21][22][23] and many more high end applications. Several improvements have been made by researchers in geometry, materials, insulators and fabrication to make the device more reliable in performance issues and still it is needed to be improving to implement in basic electronic circuitry.

Numerical simulation is very useful in understanding the sub threshold characteristics and electrical properties of a device which is also helpful in designing of a better model. 2D device simulator like ATLAS from Silvaco international would be suitable for the purpose. In this paper, numerical simulation of the device is done with top and bottom gate configurations to understand how the device behaves physically.

A number of devices with different geometry were implemented in the structure of device and their performance was noted down. Pentacene organic semiconductor was used as an active layer of transistor because of its high mobility. In this paper, we model the characteristics of top and bottom gate configurations including top gate top contact (TGTC), top gate bottom contact (TGBC), bottom gate top contact (BGTC), bottom gate bottom contact (BGBC). The path of charge carriers changes in different geometries which possess difference in the electrical behavior of the devices. The performances of bottom and top gate pentacene based devices are compared and their performance parameters like mobility, threshold voltage, sub threshold slope, trans conductance, on off ratio are summarizing in detail.

1 II.

2 Experimental Setup

3 III. MODELLING AND NUMERICAL SIMULATION

4 Numerical simulation of Electrical characteristics of the top and bottom gate configuration is measured using
 5 TCAD ATLAS by Silvaco International software. TCAD ATLAS by Silvaco International is physically based,
 6 numerical device simulator which predicts the electrical behavior of device and used to design a high performance
 7 device. This section describes the simulation procedure followed by ATLAS software. This software follows some
 8 fundamental equations that are linked with performance parameters.

9 The equations used by the ATLAS to simulate the Device are Poisson's equation and
 10 Continuity equation which were used to measure the characterization of these two devices.
 11 [9][10][11][12][13][14][15][16][17][18][19][20][21][22][23]

4 a) Poisson's equation

5 Poisson's Equation relates variations in the electrostatic potential to local charge densities. It is mathematically
 6 described by the following relation [9][10][11][12][13][14][15][16][17][18][19][20][21][22][23], $\nabla^2 \phi = -\rho / \epsilon$ (1)

7 Where ϕ is the electrostatic potential, ρ is the local space charge density, ϵ is the local permittivity of the
 8 semiconductor (F/cm), p is the hole density (cm⁻³), n is the electron density (cm⁻³), N_d is the ionized
 9 donor density (cm⁻³) and N_a is the ionized acceptor density (cm⁻³). The reference potential is always
 10 taken as the intrinsic Fermi potential for simulations in ATLAS. The local space charge density is the sum of all
 11 contributions from all mobile and fixed charges, including electrons, holes and ionized impurities.

5 b) Continuity Equations

6 For electrons and holes, the continuity equations are defined as follows:
 7 $\nabla \cdot J_n + G_n - R_n = \partial n / \partial t$ (3)
 $\nabla \cdot J_p + G_p - R_p = \partial p / \partial t$ (4)

6 c) Transport Equations

7 These equations are to specify the physical models for electrons and holes current densities and generation
 8 (recombination) rates. The Current density equations are obtained by using the "drift-diffusion" charge transport
 9 model. The reason for this choice lies in the inherent simplicity and the limitation of the number of independent
 10 variables to just three, n and p . The accuracy of this model is excellent for all technologically feasible feature
 11 sizes. The drift-diffusion model is described as follow:
 $J_n = q n \mu_n E + q D_n \nabla n$ (5)
 $J_p = q p \mu_p E - q D_p \nabla p$ (6)

12 where n and p are the electron and hole concentrations, J_n and J_p are the electron and hole current densities,
 13 G_n (R_n) and G_p (R_p) are the generation (recombination) rates for the electrons and holes, respectively and
 14 q is the fundamental electronic charge. ATLAS incorporates both eqns. In simulations, but, also gives the user
 15 an option to turn off one of the two equations and solve either the electron continuity equation.

16 where μ_n and μ_p are the electron and hole mobilities, D_n and D_p are the electron and hole diffusion
 17 constants, E_n and E_p are the local electric fields for electrons and holes, respectively, and ∇n and ∇p are the
 18 three dimensional spatial gradient of n and p . The local electric fields are defined as follows:
 $E_n = -\nabla \phi - (kT/q) \nabla \ln n$ (7)
 $E_p = -\nabla \phi - (kT/q) \nabla \ln p$ (8)

19 Where n_{ie} is the local effective intrinsic carrier concentration.

20 For numerical simulation of OTFT device with top and bottom gate configuration, the Poole-Frenkel mobility
 21 model has been employed for Pentacene active channel and defines the dependency of mobility capability due to
 22 electric field, this model is expressed as [20][21][22][23], $\mu = \mu_0 \exp(-E_C/kT) \exp(\beta \sqrt{E})$ (9)

23 Here, in equation (9), μ_0 is zero field mobility, F is electric field, and β is characteristic parameter for the
 24 field dependence.

IV.

7 The Density of Defect States

8 The density of the defect states (DOS) $g(E)$, which dominates the properties of amorphous or polycrystalline
 9 TFTs, is modeled as a combination of four components [3], where E denotes the state energy.

10 The equations describing these terms are given as follows [8] $g(E) = N_{TA} \exp(-(E - E_C)/kT) + N_{TD} \exp(-(E_C - E)/kT) + N_{GA} \exp(-(E - E_V)/kT) + N_{GD} \exp(-(E_V - E)/kT)$ (10)
 11 $g(E) = N_{TA} \exp(-(E - E_C)/kT) + N_{TD} \exp(-(E_C - E)/kT) + N_{GA} \exp(-(E - E_V)/kT) + N_{GD} \exp(-(E_V - E)/kT)$ (11)
 12 $g(E) = N_{TA} \exp(-(E - E_C)/kT) + N_{TD} \exp(-(E_C - E)/kT) + N_{GA} \exp(-(E - E_V)/kT) + N_{GD} \exp(-(E_V - E)/kT)$ (12)
 13 $g(E) = N_{TA} \exp(-(E - E_C)/kT) + N_{TD} \exp(-(E_C - E)/kT) + N_{GA} \exp(-(E - E_V)/kT) + N_{GD} \exp(-(E_V - E)/kT)$ (13)

14 where E is the trap energy, E_C is conduction band energy, E_V is valence band energy, and the subscripts T, G,
 15 A, D stand for tail, Gaussian (deep level), acceptor and donor states respectively. The exponential distribution of
 16 DOS is described by conduction and valence band intercept densities (N_{TA} and N_{TD}), and by its characteristic
 17 decay energy (W_{TA} and W_{TD}). For Gaussian distributions, the DOS is described by its total density of states

101 (N GA and N GD), its characteristic decay energy (W GA and W GD), and its peak energy/peak distribution
 102 (E GA and E GD).

103 Input parameters used in the simulation of the OTFT devices with different geometries are summarized in Table
 104 ??I. V. RESULTS AND DISCUSSIONS All Organic thin film transistor devices were built up with technique of
 105 top gate and bottom gate configuration with top and bottom contacts. Electrical characterization and numerical
 106 simulation of the devices are measured using TCAD ATLAS by Silvaco International software and with the of
 107 characterization of devices, electrical performance parameters such as Mobility, Trans conductance, threshold
 108 voltage, Sub threshold sweep and on/off ratio were calculated.

109 Mobility is the rate of flow of charge carriers in the electric field. It is the parameter which deals with processing
 110 speed of device. This mobility (μ) has been calculated using the following equations, $\mu = (L \times g_m) / (W \times C_{ox} \times V_{ds})$ (10) $g_m = dI_{ds} / dV_{gs}$ (11) $C_{ox} = \epsilon_{ox} / d_{ox}$ (12) Here, g_m is the trans conductance which is
 111 calculated by transfer characteristics curve (I_{ds} / V_{ds}) and calculation is done by equation (11). L and W are
 112 length and width of device respectively. C_{ox} is the capacitance of oxide with is the ratio of permittivity of oxide
 113 and thickness of oxide, given by equation (??2). V_{ds} is drain voltage which is taken as 1V for all the devices.

114
 115 Minimum From above calculation, it was observed that bottom gate configuration perform better than top
 116 gate configuration in terms of mobility, sub threshold slope and with good on off ratio but top gate configuration
 117 have higher on off ratio as compared to bottom gate configuration which is in magnitude of 10^8 .

118 8 VI. CONCLUSION

119 This paper presented the numerical simulation and characterization of bottom and top gate pentacene based
 120 OTFTs. The performances of these devices have been analyzed and their performance parameters like mobility,
 121 threshold voltage, sub threshold slope, trans conductance, on off ratio have been extracted and compared. It
 122 was observed that bottom gate configuration perform better than top gate configuration in terms of mobility,
 123 sub threshold slope and with good on off ratio but top gate configuration have higher on off ratio as compared
 124 to bottom gate configuration which is in magnitude of 10^8 .

125 9 Global Journal of Researches in Engineering () Volume XIX 126 Issue III Version I

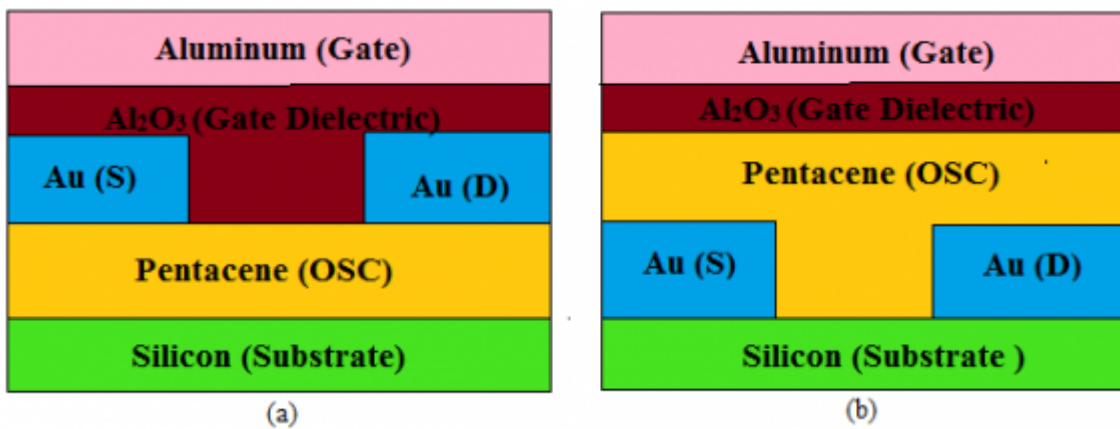


Figure 1:

127 1

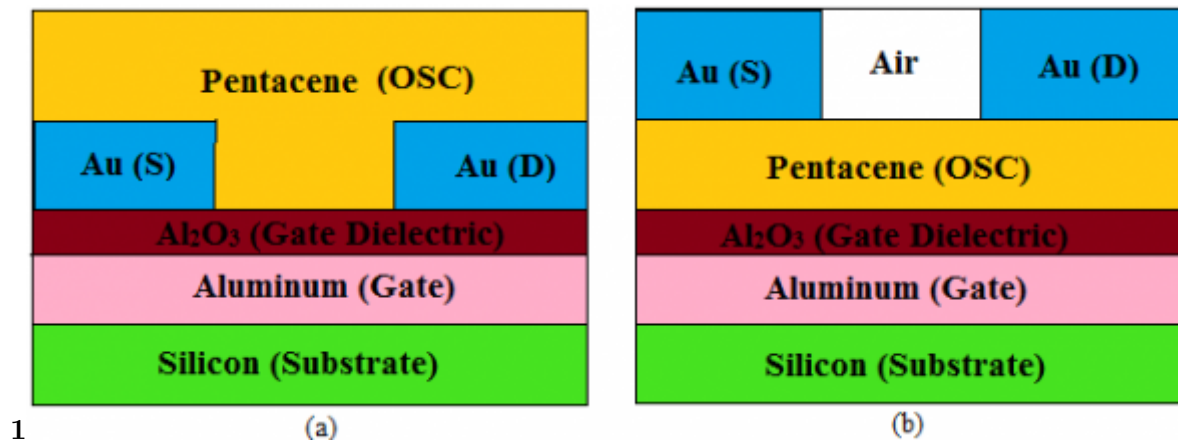


Figure 2: Fig. 1 :

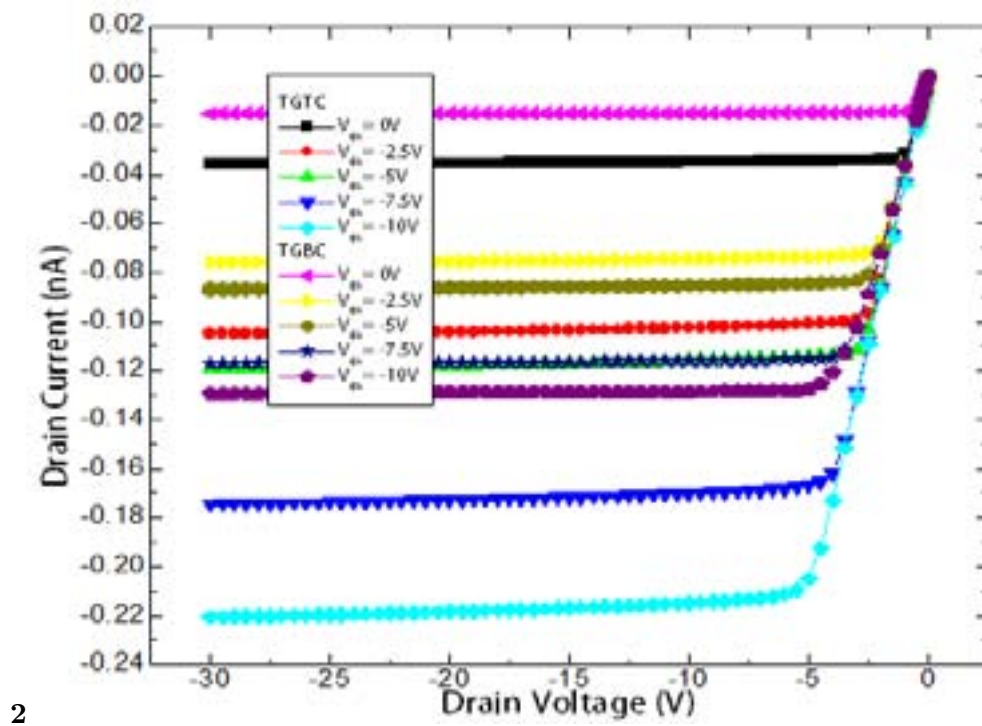


Figure 3: Fig. 2 :

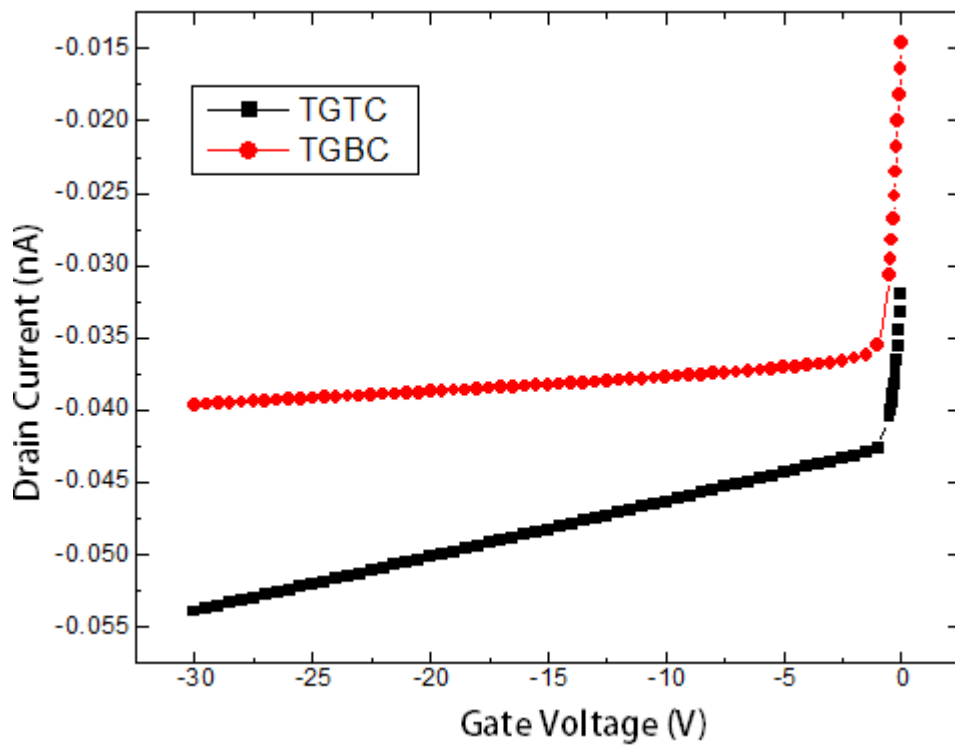
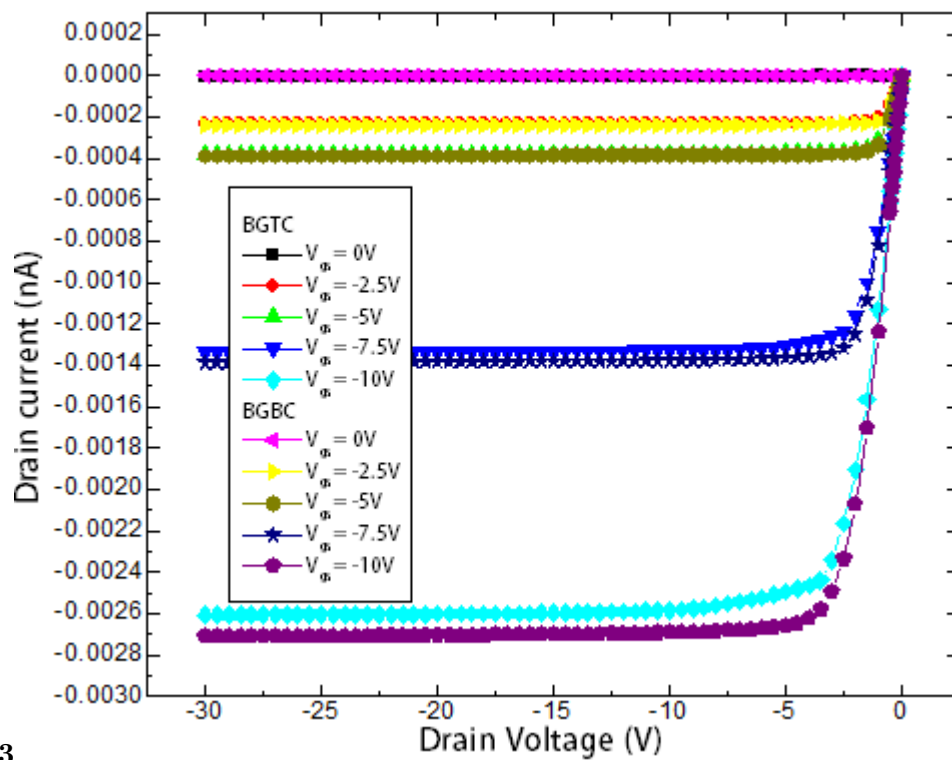


Figure 4:



23

Figure 5: Fig. 2 :Figure 3

1

Device Parameter	Value (μm)
Channel Width (W)	220
Channel length	10
Gate thickness. T G	0.02
Dielectric thickness, t ox	5.7×10^{-3}
Organic semiconductor thickness, t osc	0.03
S/D contact thickness, t c	0.03

Figure 6: Table 1 :

2

Parameters	Effective density of state in conduction band(N_c)	Effective density of state in valence band	Dielectric constant for , Al ₂ O ₃	Electron gap at 300K	N TD band	N TA	W TD	W TA	W GA
Values	$1.0 \times 10^{21} \text{ cm}^{-3}$	$8.5 \times 10^{18} \text{ cm}^{-3}$	2.8	$1.0 \times 10^{21} \text{ cm}^{-3} / \text{eV}$	$1.0 \times 10^{21} \text{ cm}^{-3}$	$2.5 \times 10^{18} \text{ cm}^{-3} / \text{eV}$	0.5eV	0.129eV	0.15eV

Year 2019
9
Global Journal of Researches in Engineering () Volume XIX Issue III Version I F

Figure 7: Table 2 :

3

Parameters	Structures			
	BGBC	BGTC	TGBC	TGTC
V t (V)	1.1		1.2	0
On off ratio	1.9×10^4		9.5×10^3	1.9×10^8

Figure 8: Table 3 :

.1 ACKNOWLEDGEMENT

- 128
129 The authors are thankful to SERB, DST Government of India for the financial support under Early Career
130 Research Award (ECRA) for Project No.ECR/2017/000179.
- 131 [Nall ()], Graciella Nall. *Organic Electronics* 81157-27-5, 2011. (First edition ISBN 978-93-)
- 132 [Garnier et al. ()] ‘An all-organic soft thin film transistor with very high carrier mobility’. F Garnier, G Horowitz
133, Z Peng, X, D Fichou. *Adv. Mater* 1990. 2 (12) p. .
- 134 [Nausieda et al. (2008)] ‘An Organic Active-Matrix Imager’. K Nausieda, I Ryu, A Kymissis, V Ibitayo
135 Akinwande, C G Bulovic, Sodini. *IEEE Transactions on Electron Devices*, Feb. 2008. 55 p. .
- 136 [Kane et al. (2000)] ‘Analog and digital circuits using organic thin-film transistors on polyester substrates’. M G
137 Kane, J Campi, M S Hammond, F P Cuomo, B Greening, C D Sheraw, J A Nichols, D J Gundlach, J
138 R Huang, C C Kuo, L Jia, H Klauk, T N Jackson. *IEEE Electron Device Letters*, Nov. 2000. 21 p. .
- 139 [ATLAS User’s Manual from SILVACO International] *ATLAS User’s Manual from SILVACO International*,
- 140 [Ha et al. (2012)] ‘Characteristics of High-Performance Ambipolar Organic Field-Effect Transistors Based on a
141 Diketopyrrolopyrrole-Benzothiadiazole Copolymer’. T J Ha, P Sonar, S P Singh, A Dodabalapur. *IEEE*
142 *Transactions on Electron Devices*, May 2012. 59 p. .
- 143 [Takamiya ()] ‘Design for Mixed Circuits of Organic FETs and Plastic MEMS Switches for Wireless Power
144 Transmission Sheet’. M Takamiya. *2007 IEEE International Conference on Integrated Circuit Design and*
145 *Technology*, (Austin, TX) 2007. p. .
- 146 [Bentes et al. ()] ‘Detection of explosive vapors using organic thinfilm transistors’. E Bentes, H L Gomes, P
147 Stallnga, L Moura. *Proceedings of IEEE Sensors*, (IEEE Sensors) 2004. 2 p. .
- 148 [Petrosino et al. ()] ‘Effects of the polymeric dielectric on OTFT performances’. M Petrosino, A Rubino, R
149 Miscioscia, A De Girolamo, Del Mauro, C Minarini. *3rd International Conference on Signals, Circuits and*
150 *Systems (SCS)*, (Medenine) 2009. 2009. p. .
- 151 [Cui et al. ()] ‘Fabrication of pentacene organic field-effect transistors containing SiO₂ nanoparticle thin film
152 as the gate dielectric’. Tianhong Cui, Guirong Liang, Jingshi Shi. *IEEE International Electron Devices*
153 *Meeting*, (Washington, DC, USA) 2003. 2003. p. .
- 154 [Kato et al. ()] ‘High mobility of pentacene field-effect transistors with polyimide gate dielectric layers’. Y Kato
155, S Iba, R Teramoto, T Sekitani, T Someya, H Kawaguchi, T Sakurai. *Appl. Phys. Lett* 2004. 84 (19) p. .
- 156 [Someya Yusaku et al. (2005)] ‘Integration of organic FETs with organic photodiodes for a large area, flexible,
157 and lightweight sheet image scanners’. T Someya Yusaku, Shingo Kato, Yoshiaki Iba, Tsuyoshi Noguchi,
158 Hiroshi Kawaguchi and Takayasu Sekitani, Sakurai. *IEEE Transactions on Electron Devices*, Nov. 2005. 52
159 p. .
- 160 [Someya ()] ‘Integration of organic field-effect transistors and rubbery pressure sensors for artificial skin
161 applications’. T Someya. *IEEE International Electron Devices Meeting*, (Washington, DC, USA) 2003. 2003.
162 p. .
- 163 [Takamiya et al. ()] ‘Low Power and Flexible Braille Sheet Display with Organic FET’s and Plastic Actuators’.
164 M Takamiya, T Sekitani, Y Kato, H Kawaguchi, T Someya, T Sakurai. *2006 IEEE International*
165 *Conference on IC Design and Technology*, 2006. Padova. p. .
- 166 [Mijalkovic (2008)] ‘Modelling of organic field-effect transistors for technology and circuit design’. S Mijalkovic.
167 *26th International Conference on Microelectronics (MIEL)*, (Nis, Serbia) May 11-2008. 14 p. .
- 168 [Dwivedi ()] ‘Numerical Simulation and Spice Modeling of Organic Thin Film Transistors (OTFTs)’. D D Dwivedi
169. *International Journal of Advanced Applied Physics Research* 2014. 1 p. .
- 170 [Dwivedi et al. ()] ‘Numerical simulation of P3HT based Organic Thin Film Transistors (OTFTs)’. A D D
171 Dwivedi, Rajeev Dhar Dwivedi, Raghendra Dhar Dwivedi, Sumit Vyas, P Chakrabarti. *International*
172 *Journal of Microelectronics and Digital integrated circuits* 2015. 1 (2) p. .
- 173 [Spanu et al. ()] ‘Organic FET device as a novel sensor for cell bioelectrical and metabolic activity recordings’. S
174 Spanu, P Lai, A Cosseddu, M Bonfiglio, S Tedesco, Martinoia. *6th International IEEE/EMBS Conference*
175 *on Neural Engineering (NER)*, (San Diego, CA) 2013. 2013. p. .
- 176 [Halik et al. ()] ‘Polymer gate dielectrics and conducting polymer contacts for high performance organic thin
177 film transistors’. M Halik, M, H Klauk, U Zschieschang, G Schmid, W Radlik, W Weber. *Adv. Mater*
178 2002. 14 (23) p. .
- 179 [Shen et al. ()] ‘SPICE Library for Low-Cost RFID Applications Based on Pentacene Organic FET’. S Shen, R
180 Tinivella, M Pirola, G Ghione, V Camarchia. *6th International Conference on Wireless Communications*
181 *Networking and Mobile Computing (WiCOM)*, (Chengdu) 2010. 2010. p. .
- 182 [Vaidya et al. (2009)] ‘SPICE Optimization of Organic FET Models Using Charge Transport Elements’. V Vaidya
183, J Kim, J N Haddock, B Kippelen, D Wilson. *IEEE Transactions on Electron Devices*, Jan. 2009. 56 p. .

- 184 [Itoh et al. ()] ‘The use of high K dielectric thin film prepared by RF sputtering as insulating layers for organic
185 TFT devices’. E Itoh , T Murayama , T Highchi , K Miyairi . *Proceedings of the IEEE International Conference*
186 *on Solid Dielectrics*, (the IEEE International Conference on Solid Dielectrics) 2004. 2004. 2004. 1 p. .
- 187 [Michaelson] ‘The work function of the elements and its periodicity’. H B Michaelson . *J. Appl. Phys* 1977 (11)
188 p. .